Seven Level T-Type Switched Capacitor Inverter Topology For PV Applications

Saeed Alyami[1], Member, IEEE, Jagabar Sathik M[2], Senior Member, IEEE, Dhafer Almakhles[2], Senior Member, IEEE, Abdulaziz Almutairi[1], Member, IEEE, Mohammed Obeidat[3], Member, IEEE,

[1]Department of Electrical Engineering, Majmaah University, 11592, Riyadh, Saudi Arabia
[2]Renewable Energy Lab, Prince Sultan University, 11586, Riyadh, Saudi Arabia.
[3]Department of Power and Mechatronics, Tafila Technical University,66110 Tafilah Jordan

*Corresponding author: Saeed Alyami (Almajmaah 11592, Riyadh, Saudi Arabia. email: s.alyami@mu.edu.sa)

ABSTRACT The conventional neutral point clamped multilevel inverter requires voltage balancing circuits or control to balance the dc-link capacitors. The same type of inverter also requires a high number of components. Since the output voltage is half of the input voltage, the size of the source side dc/dc converter in PV applications increases. In this paper, a new topology of seven level neutral point clamped inverters is developed. The proposed inverter has a self-voltage boosting capability using a floating capacitor to boost the output voltage one and half of the input voltage. In this proposed topology, no additional sensors are required for the floating capacitor voltage stability, which results in minimizing the complexity of designing the inverter. The direct link between the neutral point and the mid-point of the dc-link capacitors significantly reduces the leakage current and common mode voltage in this inverter. A thorough comparison between the developed topology and recent suggested topologies is carried out which set the benchmark for the proposed one due to its lower switch count and higher voltage gain. The proposed topology is verified in simulation and prototype hardware model and results are discussed with dynamic load variations. The efficiency of the inverter is 97.1% @200W and low as 88.1% @ purely inductive load. The voltage THD is 17.01% for simulation and 19.3% from the experimental results.

INDEX TERMS Switched capacitor circuits, seven level inverter, ANPC type, Voltage boosting, self-voltage balancing

I. INTRODUCTION

The huge demand of the energy, high cost of the fossil fuels and the environmental concerns have led to the investment and research in the other possible resources of energy, namely, renewable energy. The renewable energy resources like photovoltaic (PV) and wind energy have given good alternatives to the conventional fossil fuel. These renewable energy resources can be efficiently used in many fields of applications as a replacement of the conventional resources of energy. Power electronic converters play an integral part in the renewable energy systems. Various categories of power electronic converters have been designed for the efficient and reliable power conversion which is necessitated due to the requirement of different applications. As the output of the most of the renewable resources are dc, the inverters are often integrated between renewable energy resources and ac loads [1–4]. Thus, the use of multilevel inverters has increased significantly in the last decade due to their advantages like high quality output voltage waveforms and low voltage stresses. These attractive features have received more attention from the researcher to further improve the topology structure, reduction of components, etc.

Among several multilevel inverter topologies, the neutral point clamped (NPC), and floating capacitor (FC) topologies utilize

a single dc source with several dc-link capacitors [5–7]. NPC topology suffers from the higher number of clamping diodes, balancing of dc-link capacitors (>3L) and non-uniform power distribution of the switches. In order to resolve the drawback of NPC topology and to utilize the advantage of it, new ANPC topologies are developed. The FC of ANPC topology is balanced with or without sensors. The ANPC topology provides uniform power loss distribution and more precision control of the load [8]. Nevertheless, the ANPC output voltage is half of the input voltage (v_{in}) and it exhibits the same characteristics of NPC. To increase the output voltage without adversely affecting the natural phenomena of ANPC, new topologies for switched capacitor multilevel inverters are proposed in [9–16]. A generalized structure of the switched capacitor multilevel inverter with self-voltage balancing is presented in [9]. In this a single dc source is used to boost output voltage based on the number of switched capacitor cells. However, this topology needs more power components and the voltage stress on the switches are high, which in turn limits the medium and high voltage applications. In [10], a novel switched capacitor multilevel inverter structure is developed. This topology is configured in both symmetrical and asymmetrical mode, by extending the switched capacitor cell. The number of components is minimized but the voltage stress on the switch is increased. Another topology with self-balancing and boosting capability is proposed in [11]. The topology uses eight switches and two diodes with a voltage
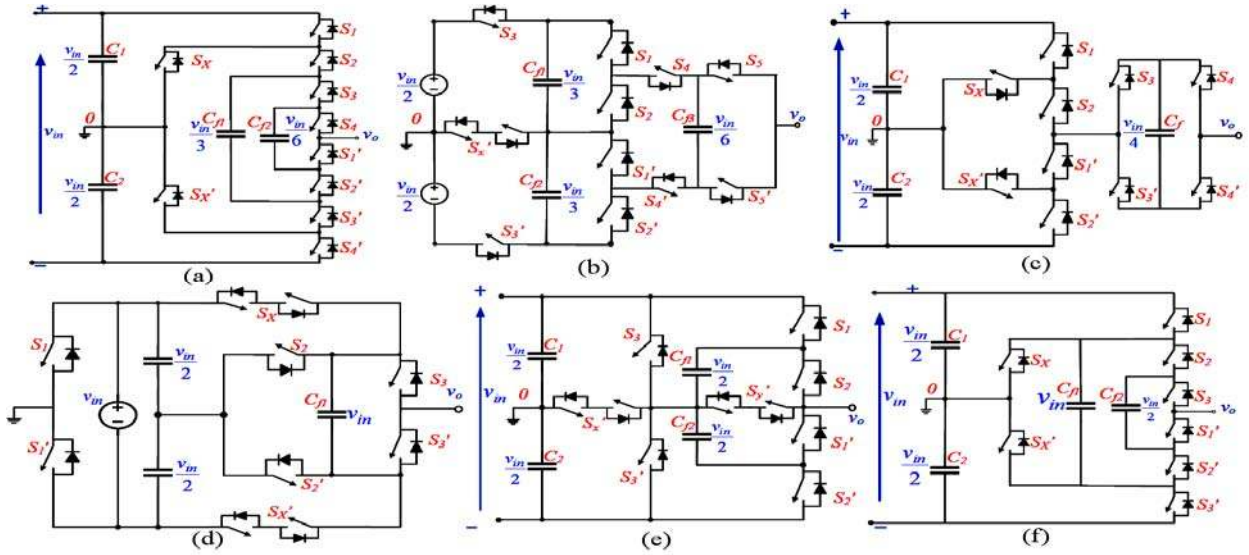
FIGURE 1 Multilevel Inverter Topologies (a) Topology 7L-ANPC [13], (b)Hybrid 7L-ANPC [14] (c) Hybrid 7L-ANPC-III [15], (d) 7L-SCMLI [16], (e) Topology DTT-7L-BANPC [17] and (f) 7L-Boost-ANPC [18]
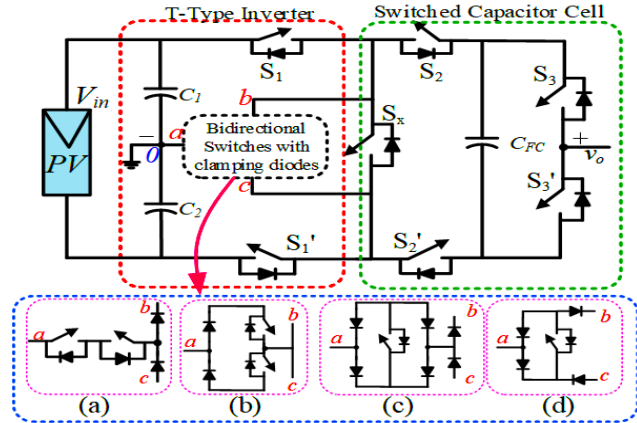
FIGURE 2 Proposed Boost Active Neutral Point Clamped T-Type 7L Switched Capacitor Inverter (BANPC T-7LSCI), (a) –(c) various bidirectional switch (Bx) and (d) proposed bidirectional switch (Bx)

boosting of 1:3. Since the diode is presented in the main current path, the topology is not suitable for high inductive load applications. To overcome the stress on full bridge inverter switches, a cascaded topology is recommended, but the use of a number of dc sources and other components are increased. These topologies are extendable to "*m*" number units and the voltage stress on the switch is also proportionally increasing. The output voltage is boosted to 1.5 times of v_{in} and presented in [12]. Voltage and current sensors are used to measure the change of voltage in a FC and direction of load current. Further, logic form equation methods are implemented to select the appropriate levels based on the sensor output. This increases the complexity of the controller and reduces the reliability of the inverter because the whole operation depends on the sensor's output. In order to resolve the above problems seven level topology with compact components and voltage stress on switches are presented in [13–24] and the recently innovated topologies are shown in Fig. 1(a)-(f).

In Fig.1 (a)-(c), the topologies are hybrid of the ANPC and FC structure. The structure uses two different voltage ratings of dc-link capacitors and the capacitor voltages are regulated by additional sensors. The output voltage of the inverter is always half of the input voltage (v_{in}). The boost converter topologies are shown in Fig.1 (d)-(f), where the output of these topologies

is equal or higher than the input voltage. However, these topologies are suffering from high voltage stress and more power components. For less components, low voltage stress in a new boost active neutral point clamped T-Type 7- Level inverter (BANPC T-7L) topology is proposed in this paper.

II. PROPOSED BANPC T-7L INVERTER TOPOLOGY

Fig.2 comprises two dc-link capacitors (C_1 & C_2), one FC and nine switches (S_1-S_3, S_1'-S_3', B_x & S_x) with two diodes. The combination of a T-type and switched capacitor cell form the proposed 7L inverter topology. In the T-type inverter, the neutral point is taken at the mid-point of the series connected dc-link capacitors. The voltage across the dc-link capacitors C_1 & C_2 is $v_{in}/2$ and the voltage across the FC is equal to the input voltage (v_{in}). The upper capacitor C_1 is supplying the power in the first half cycle and C_2 in the second half cycle.

The proposed BANPC T-7L inverter topology has the following advantages:

i)   Less power components
ii) Self-voltage balancing of floating capacitor (FC)
iii) Output voltage (v_o) is 1.5 times higher than v_{in}.
iv) The FCdo not depend on the load power factor

IEEEAccess

Saeed A, J. Sathik, D. Almakhles, Abdulaziz A, Mohammed O
Seven Level T-Type Switched Capacitor Inverter-Rooftop PV Applications

v)   Less leakage current since the neutral point is linked to

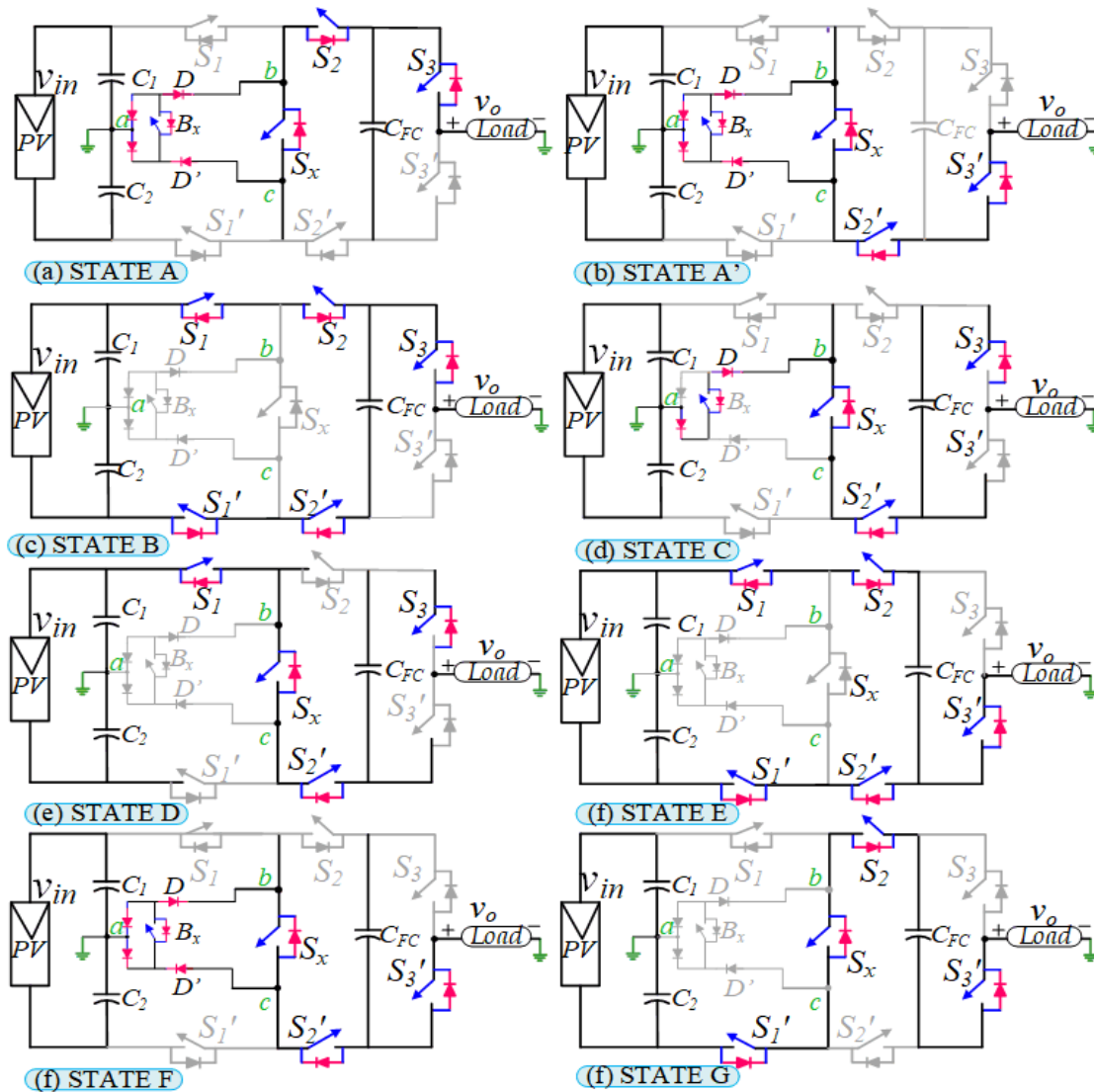bidirectional switch is used which further reduces the two

FIGURE 3 Operation modes of BANPC (a)-(h) different current path of each voltage level

the mid-point of the dc-link capacitor.

vi)   No additional circuits or sensors are needed for capacitors stability.

vii) Appropriate choice for transformerless grid connected PV system.

TABLE I
SWITCHING SEQUENCE AND CORRESPONDING STATES FOR BANPC T-7LSCI

States	ON State Switches	ΔV_{FC}	V_o
STATE A	$B_X, S_X D, D', S_2 S_3$	-	$0\ v_{in}$
STATE A'	$B_X, S_X D, D', S_2', S_3'$	-	
STATE B	$S_1, S_2, S_1', S_2', S_3$	▲	$+v_{in}/2$
STATE C	$B_X, S_X D, S_2', S_3$	▼	$+v_{in}$
STATE D	S_1, S_X, S_2', S_3	▼	$+3v_{in}/2$
STATE E	$S_1, S_2, S_1', S_2', S_3'$	▲	$-v_{in}/2$
STATE F	$B_X, S_X D', S_2', S_3$	▼	$-v_{in}$
STATE G	S_1', S_X, S_2, S_3'	▼	$-3v_{in}/2$

▲ - Charging of FC,   ▲ - Discharging of FC

The switching sequence and corresponding output voltage is listed in Table I. In that proposed topology fig.2 (d)

diodes.   The various output voltage levels along with the current paths are shown in Fig. 3 (a)-(h).

Mode (0v$_{in}$): Fig. 3(a) & (b) show the state A and A' and it provides the continuous current path in the zero-voltage level. The switches *Bx* and *Sx* are conducting through the diode *D* and *D'* with S_2 & S_3 as given in Table I.

Mode (+v$_{in}$/2): The output voltage v_{in} /2, i.e both dc-link capacitors charge the FC through switches S_1, S_2, S_1' & S_2' and half of the input voltage $v_{in}/2$ is tapped to the load through S_3 as shown in Fig. 3 (c) and State B given in Table. I.

Mode (+v$_{in}$): In State C, the output voltage is equal to the input voltage and FC is discharged through the switches *Bx, Sx, S_2'* & S_3 as shown in Fig. 3 (d).

Mode (+3v$_{in}$/2): The output voltage v_o is 1.5 times higher than v_{in}. It is obtained by adding the voltages of the upper capacitor (V_{C1}) and (V_{FC}). The corresponding switches S_1, Sx, S_2' & S_3 are turned ON as shown in Fig. 3(e). Similarly, in the negative half cycle the FC is charged and discharged as shown in Fig. 3 (f)-(h). However, the maximum number conducting switches is

five, which reduces the switching and conduction losses compared to topologies presented in [13]–[18].

The voltage and current stress of the proposed BANPC topology are given in Table II and III respectively. The switches S_1, S_1', and B_x need to block a voltage equal to half of the input voltage, i.e. $v_{in}/2$. The voltage blocking of the other switches needs to be equal to input voltage i.e., v_{in}.

TABLE II
VOLTAGE STRESS OF SWITCHES

v_o	S_1	S_1'	S_2	S_2'	S_3	S_3'	B_x	S_x
$3v_{in}/2$	0	$v_{in}/2$	v_{in}	0	0	v_{in}	$v_{in}/2$	0
v_{in}	$v_{in}/2$	$v_{in}/2$	v_{in}	0	0	v_{in}	0	0
$v_{in}/2$	0	0	0	0	0	v_{in}	$v_{in}/2$	v_{in}
Zero	$v_{in}/2$	$v_{in}/2$	0	v_{in}	0	v_{in}	0	0
$-v_{in}/2$	0	0	0	0	v_{in}	0	$v_{in}/2$	v_{in}
$-v_{in}$	$v_{in}/2$	$v_{in}/2$	0	v_{in}	v_{in}	0	0	0
$-3 v_{in}/2$	0	$v_{in}/2$	0	v_{in}	v_{in}	v_{in}	$v_{in}/2$	0

TABLE III
CURRENT STRESS OF SWITCHES

v_o	S_1	S_1'	S_2	S_2'	S_3	S_3'	B_x	S_x
$3V_{in}/2$	I_o	0	0	I_o	I_o	0	0	I_o
V_{in}	0	0	0	I_o	I_o	0	I_o	I_o
$V_{in}/2$	I_o+I_c	I_o+I_c	I_o+I_c	I_o+I_c	I_o+I_c	0	0	0
Zero	0	0	I_o	0	I_o	0	I_o	I_o
$-V_{in}/2$	I_o+I_c	I_o+I_c	I_o+I_c	I_o+I_c	0	I_o+I_c	0	0
$-V_{in}$	0	0	I_o	0	0	I_o	I_o	I_o
$-3V_{in}/2$	I_o	0	I_o	0	0	0	0	I_o

I_o = Load current, and I_c = charging current

III. CAPACITOR VOLTAGE ANALYSIS

The voltage of the capacitors are affected by several factors like output power magnitude with power factor, output voltage frequency, modulation technique, etc. In the literature, several modulation techniques have been discussed for the SC- based topologies, among which the phase disposition PWM (PD-PWM) technique has been extensively used. For the proposed topology, PD-PWM has been used and is shown in Fig. 4 for a half cycle of the output voltage. To do the capacitor voltage analysis in the worst condition, the carrier signals can be replaced with some dc lines of magnitude equal to half of the carrier magnitude as shown in Fig. 4. Whe

With worst condition, the output voltage is shown in Fig. 4 along with the floating capacitor voltage V_{FC}. Fig. 5 depicts the equivalent circuit with the capacitor connection for the proposed 7L topology with positive output voltage levels. The different equations for the output voltage are given as:
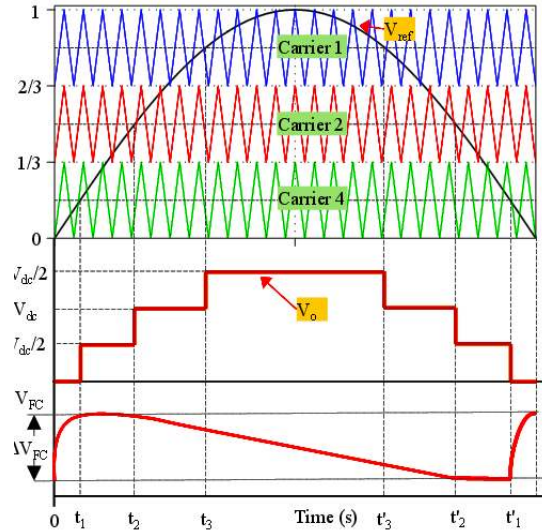

FIGURE 4 PD-PWM, output voltage and floating capacitor voltage variation of FC.
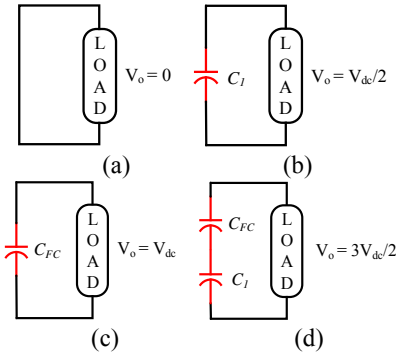

FIGURE 5 Equivalent voltage states with (a) $V_o = 0$, (b) $V_o = V_{dc}/2$, (c) $V_o = V_{dc}$ (d) $V_o = 3V_{dc}/2$

$$
\left.
\begin{aligned}
V_o &= 0 \\
V_o &= \frac{V_{dc}}{2} e^{\frac{t_2-t_1}{R_L C_1}} \\
V_o &= V_{dc} e^{\frac{t_3-t_2}{R_L C_{FC}}} \\
V_o &= \frac{3V_{dc}}{2} e^{\frac{t_3'-t_3}{R_L(C_1+C_{FC})}}
\end{aligned}
\right\} \qquad (1)
$$

where R_L = resistive load, $C_1 = C_2$ = capacitance value of dc link capacitors and C_{FC} = capacitance value of FC.

The determination of capacitance is based on the discharging duration. Here, in the second level (v_{in}) the FC continues discharging and this duration is called the longest discharging duration (LDD) as shown in Fig. 6. This LDD is taken into consideration while choosing the value of the floating capacitors. The maximum discharging and optimal capacitance for the developed inverter is expressed by

$$
Q_{FC} = 2 \times \int_{t2}^{T/4} i_o(t)\, dt \qquad (2)
$$

Where i_o is load current

IEEE *Access*

Saeed A, J. Sathik, D. Almakhles, Abdulaziz A, Mohammed O
Seven Level T-Type Switched Capacitor Inverter-Rooftop PV Applications

A. For Resistive Load (RL):

The load current during the level 2 and level 3 w.r.t to time period is expressed in (3)

$$i_o(t) = \begin{cases} \dfrac{v_{in}}{R_L} & t_2 \le t \le t_3 \\ \dfrac{3v_{in}}{2 \times R_L} & t_3 \le t \le \dfrac{T}{4} \end{cases}$$

(3)

where t_3 and t_2 equal $3T/16$ and $T/8$, respectively. The optimal capacitance for the FC with the highest acceptable voltage ripple is

$$Optimum_{Cap} \ge \frac{Q_{FC}}{k \times v_{in}}$$

(4)

where "k" is the FC ripple factor which lies between 0 to 1. Considering (2), (3), and (4) yields the optimal FC value as

$$Optimum_{Cap}, FC \ge \frac{5\pi}{8R_L \times k \times \omega \times v_{in}}$$

(5)

B. For Resistive-Inductive Load:

Considering the inductive loading condition, the load current is expressed as

$$i_o(t) = I_m Sin(\omega t - \varphi)$$

(6)

where I_m is maximum load current, φ-is phase angle between voltage and current. Therefore, by applying (2), (3) & (6) in to (4), the optimum capacitance is obtained from (7)

$$Optimum_{Cap}, FC \ge \frac{2 I_m}{k \times \omega \times v_{in}} \left[cos\left(\frac{\pi}{4} - \varphi \right) - sin(\varphi) \right]$$

(7)

From the above equations (4) and (6) it can be seen that the optimum capacitance value is inversely proportional to the voltage ripple factor (k) and frequency ($\omega=2\pi f$). In Fig. 7, the optimum capacitance value for various resistive loads is shown for constant load current.

### C. Power Loss Analysis
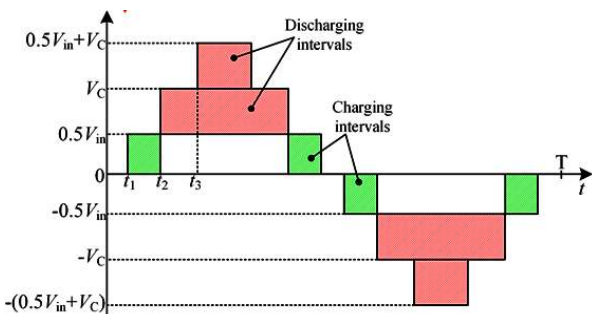
FIGURE 6 A typical seven level output voltage waveform of fundamental switching scheme

With the association of power semiconductor devices to a converter topology, two types of losses occur with them, i.e., conduction losses and switching losses. The overall power loss of the power semiconductor device is given as

$$P_{loss} = P_c + P_{sw}$$

(8)

Where Ploss represents the total power loss of the device, Pc amounts the conduction losses and Psw shares the switching
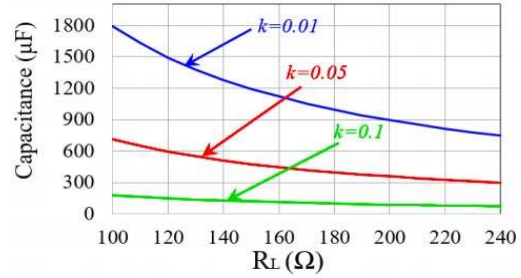
FIGURE 7 Optimum capacitance Value for various resistive load

loss of the Ploss. The conductor losses within a device occur due to the power loss of the internal resistance. The conduction losses can be calculated as

$$P_c = \sum_{allswitches} I_{o,switch}^2 R_{on}$$

(9)

Where $I_{o,switch}$ gives the current flow through each device and R_{on} is their internal resistance during the ON state of the device.

The other major losses are the switching losses. Switching losses take place in a power semiconductor device due to the intrinsic switching delays. Due to this, the voltage and current has a certain value and they overlap each other, results in the switching loss of the device which is given as

$$P_{sw} = \left[\sum_{allswitches} \sum_{within \, 1/f_o} \frac{V_{on}I_{on}T_{on}}{6} + \frac{V_{off}I_{off}T_{off}}{6} \right] \times f_o$$

(10)

Where Von, Ion, and Ton are the on-state quantities of voltage, current and time over the on-transition period respectively. Voff, Ioff, and Toff are the off-state quantities of voltage, current and time over the off-transition period respectively. fo represents the frequency of the output voltage waveform.

D. Comparison with Other Recent ANPC Topologies

In Table IV, the proposed 7L topology is compared with recent multilevel inverters using switched capacitors. A comparison for number of switches, (N_{Switch}), number of diodes (N_{Diode}), number of floating capacitors (N_{FC}), maximum voltage rating of floating capacitor (MV_{FC}) and maximum blocking voltage (MB V) on the switch is presented. Further, the maximum voltage on switches in terms of output voltage (H) and output voltage gain (G) is presented. The topologies [9–11] uses a full bridge inverter circuit at the output having a voltage stress which is 3 times higher than the input voltage. In [12], the topology uses single dc source and no neutral mid-point. The topology needs voltage and current sensors to balance the FC and it decreases the reliability and increases the complexity of the system. The output voltage is half of the input voltage but the uneven loss distribution is resolved in [13]. The topology with three floating capacitors and different voltage ratings are used [14] and sensors are required to balance the floating capacitors. In [15], the topology is developed for a 7L output voltage waveform. The FC voltage is

TABLE IV
COMPARISON WITH OTHER RECENT SCMLI TOPOLOGIES [9]-[18]

| Topologies	N_{Switch}	N_{Diode}	N_{FC}	N_{ON-Sw}	MV_{FC}	MBV	H=MBV/v_o	G=v_o/v_{in}	Family of NPC	Remarks
[9]	7	4	2	4	v_{in}	$3 v_{in}$	1.0	1:3	No	The MBV is high.
[10]	9	1	2	5	v_{in}	$3 v_{in}$	1.0	1:3		
[11]	8	2	2	4	v_{in}	$3 v_{in}$	1.0	1:3		
[12]	9	-	1	5	$v_{in}/2$	v_{in}	0.66	1:1.5		Need sensors to balance the FC voltage
[13]	10	-	2	5	$v_{in}/2$	$v_{in}/2$	1.0	1:0.5	Yes	Number of switches are high and v_o<v_{in}.
[14]	12	-	3	5	$v_{in}/3$	$v_{in}/2$	1.0	1:0.5		Number of switches are high and v_o<v_{in}.
[15]	10	-	3	5	$v_{in}/4$	$v_{in}/2$	1.0	1:0.5		Number of switches and FCs are high and v_o<v_{in}.
[16]	10	-	3	6	v_{in}	v_{in}	0.66	1:1.5	No	Number of switches are high
[17]	10	-	2	5	v_{in}	$2 v_{in}$	1.33	1:1.5	No	High MBV and Switch Count also high
[18]	8	-	2	7	v_{in}	v_{in}	1.0	1:1	Yes	v_o=v_{in}, voltage gain is 1.
[19]	12	-	2	8	v_{in}	$2 v_{in}$	0.66	1:3	No	Switch Count is high
[24]	8	1	2	4	$2 v_{in}$	$3 v_{in}$	1.0	1:3	No	High MBV and Switch Count also high
Proposed	8	4	1	4	v_{in}	v_{in}	0.66	1:1.5	Yes	MBV equal to v_{in}, number of switches are less and 1.5v_o>v_{in}
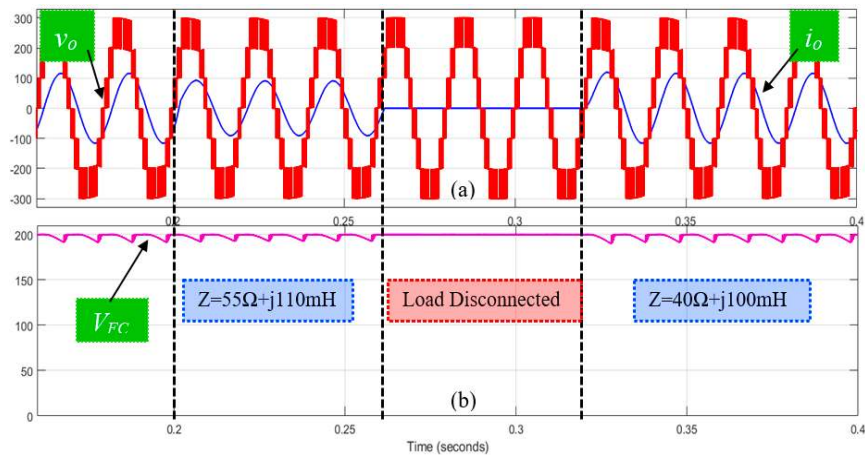
FIGURE 8 Simulation results during the dynamic load variations (a) Load voltage and current (b) the FC voltage
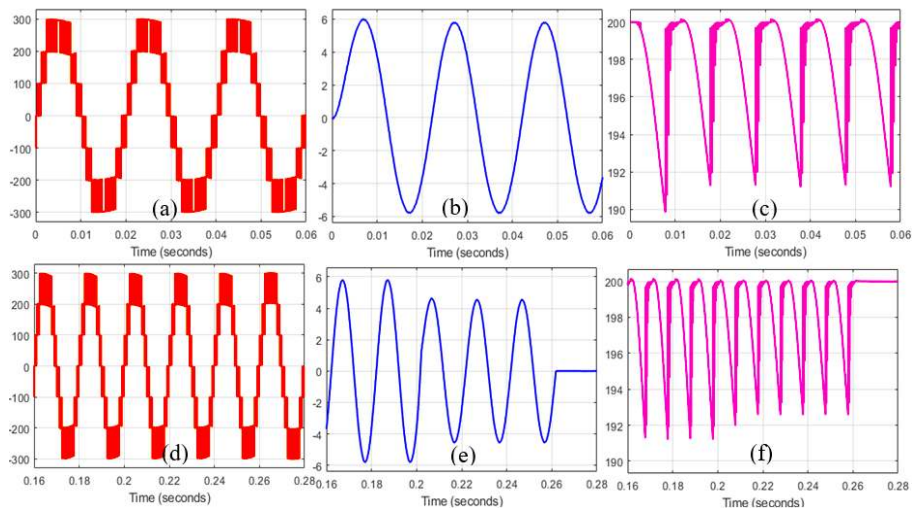

FIGURE 9 zoomed view of simulation results during the steady state and dynamic load variations (a) for steady state Load voltage (b) for steady state load current (c) for steady state FC voltage (d) dynamic load variations load voltage (e) dynamic load variations load current and (f) dynamic load variations FC voltage

lower than the input voltage and the output voltage is half of the input voltage. The FC voltage and number of switch count are high in [16] and the voltage stress is also high. Other topologies [17, 18] are suitable for transformerless inverter operation due to the neutral point being directly connected to mid-point of the dc-link capacitors.

IV. RESULTS AND DISCUSSION

A. Simulation Results of the Proposed 7L Boost Topology

The simulation of the proposed 7L BANPC has been conducted using MATLAB/Simulink software and has been discussed in the section. The different parameters used for the simulation have been listed in the Table V.

IEEE Access·

Saeed A, J. Sathik, D. Almakhles, Abdulaziz A, Mohammed O
Seven Level T-Type Switched Capacitor Inverter-Rooftop PV Applications

TABLE V
SIMULATION PARAMETERS

Component		Rating/Value
Input Voltage (v_{in})		200V
Output voltage (v_o)		300V
Capacitors (C_{FC})		2700 µF
Switching & Fundamental Frequency		2.5 kHz & 50 Hz
Resistive, Inductive	Load 1	40 Ω, 100 mH,
	Load 2	55 Ω ,110mH

FIGURE 11 Voltage and current THD for Z=55 Ω+j110 mH

The simulation results for sudden load changing waveforms are given in Fig 8 (a)-(b). In fig. 8 (a) load changing sequence of R=40 Ω & L=100 mH to R=55 Ω & L=110 mH to No-load to R=40 Ω & L=100 mH. When the load is Z=40 Ω+ j100 mH the peak output current is ~5.8A with current RMS of ~4.1A as shown in Fig. 8 (a) and after load changes occur the load current is reduced to 4.6A with current RMS 3.2 A for the power factor of (pf) 0.85. In no-load condition, the output current is zero. However, during the load change the output voltage and the FC voltage is not affected and it is evident that the proposed topology is adoptable to load variation. In Fig. 8 (b), the FC voltage ripple is little bit varying due to increasing load current and maintaining constant at no-load condition. The zoomed view of the output voltage and current during the steady state and dynamic state is shown in Fig. 9. In this the FC ripple voltage is approximately varying to maximum of 10% which is an allowable range. In normal the ripple voltage is allowable from 5% to 10%. When the v_{in} is varying the inverter circuit should maintain the output voltage level. In order to confirm the performance of the proposed inverter during the v_{in} variations is shown in Fig. 10. In this the v_{in} changed from 100V
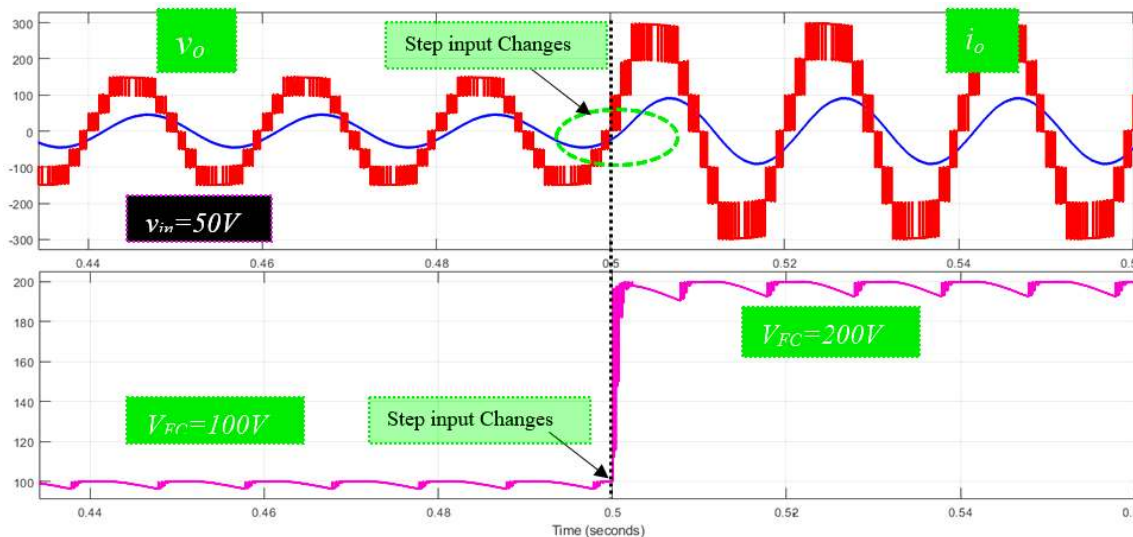
B. Experimental Results

The experimental results of the proposed 7L output voltage and current are shown in Fig. 12 (a) - (d). The experimental parameters are given in Table. VI.

TABLE VI
EXPERIMENTAL PARAMETERS

Description	Model Number	Ratings
Input voltage (v_{in})	-	200 V
Output voltage (v_o)	-	300V
Load	R-L Load Bank	2.0k W
Switches (MOSFET)	IRF640	600V/18A
Driver Circuits	TLP 250A	10-35 V/5 mA
Maximum Power @ load (P_{max})	-	~0.9 kW

In the experiment, the input voltage (v_{in}) is 200 V, the dc-link capacitors C_1 & C_2 are rated for 100V/470 µF and the rating of FC is 200V/2.7 mF. The output voltage is 300 V (v_o), which is 1.5 times higher than v_{in}. The conventional SPWM switching method is used to generate the switching pulses. The resistive

FIGURE 10 Simulation results during the v_{in} variations (a) v_{in}= 100V to v_{in}= 200V (b) the corresponding FC voltage

to 200V (i.e $V_{C1}=V_{C2}=50$V) and the output voltage level was maintained to 9L without any oscillation as shown in Fig. 10 (a). During the v_{in} changing time the FC voltage also raised from 100V to 200V as shown in Fig. 10 (b). The THD value of output voltage is 17.03% and current THD is 1.01% for the load impedance of Z=55 Ω+j110 mH as shown in Fig. 11.

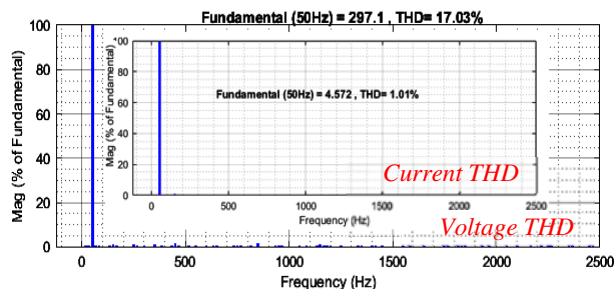and inductive loads values are 40 Ω & 100 mH, respectively. When the load is low the output current is 5.7 A (i_o) with a lagging power factor of 0.79 due to high inductive load. Sudden load change is applied from Z=40 Ω +j 100 mH to Z=55 Ω +j 110 mH to no-load the corresponding waveforms are shown in Fig. 12 (b). When the load change from low to high the output current is reduced from high to low (P_{max}= 0.7kW) as shown in Fig. 11 (b). Further the clear view of each load change is shown in Fig. 12 (c) - (d).
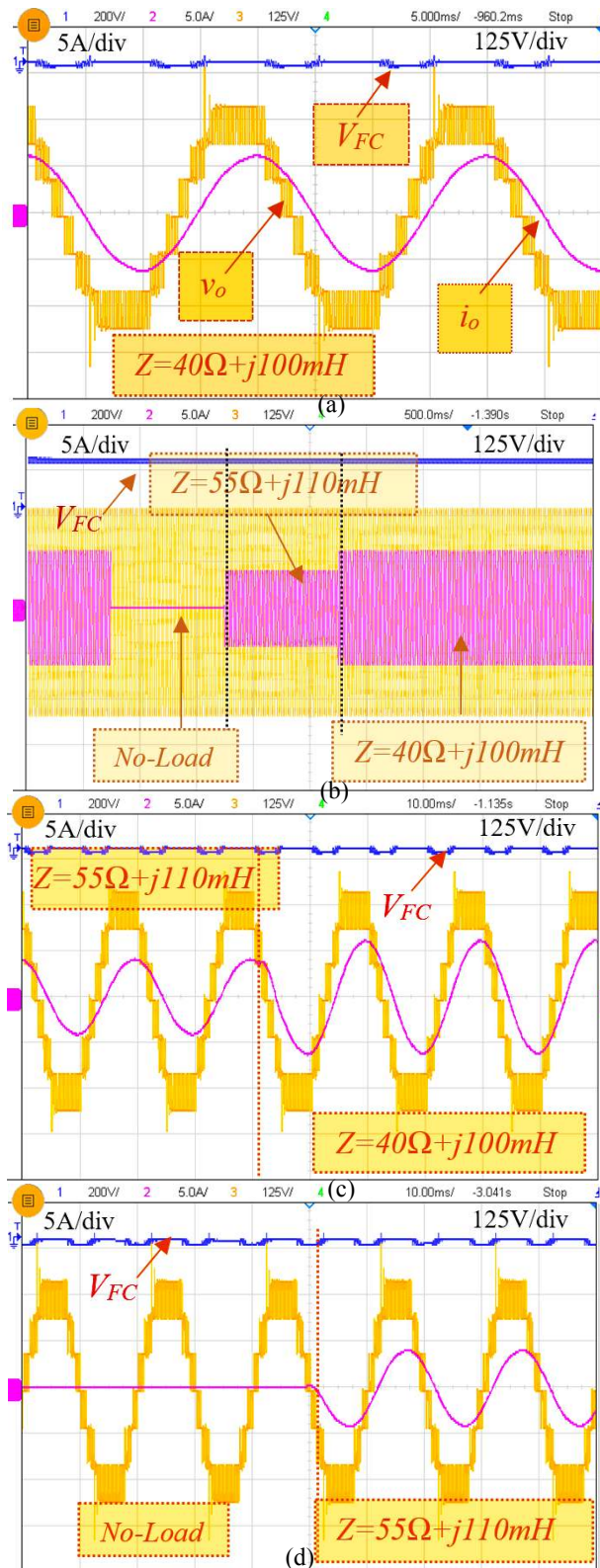
FIGURE 12 Experimental results (a) Output voltage and current (c)-(d) different load variations.

The proposed topology is tested in switching frequency of 2.5 kHz. However, during the load changes the output voltage is not affected and the floating capacitor (V_{FC}) is able to supply the energy as required by the load without any disturbance. Since at the input side two capacitors are used, which is

balancing automatically with a small ripple voltage as shown in Fig. 11 (b). The THD FFT spectrum for output voltage is shown in Fig. 13. In simulation the THD value is 19.3%.
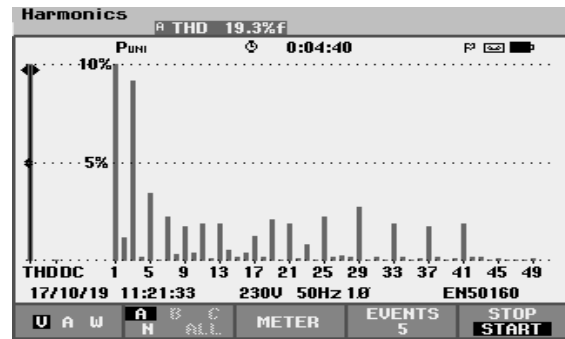

FIGURE 13 Experimental voltage FFT Spectrum

The power loss of the proposed topology has also been estimated. Fig. 14 (a) depicts the efficiency curve of the proposed topology. The maximum efficiency of the proposed topology comes out to be 97.1% with the output power of 200W. In addition, the proposed topology has significantly higher efficiency at higher output power as shown in Fig. 14 (a). Fig. 14 (b) illustrates the effect of loading on the efficiency at different loading conditions. With purely resistive load of 45Ω, the output power is 1000W with the efficiency of 95%. As the load is changed to a combination of resistive-inductive load (Z = 100mH + 50Ω), the efficiency becomes 95.2% with output power of 636.1W. Similarly, with a highly inductive load (Z = 80mH + 1Ω), the efficiency drops to 88.1% due to higher demand of reactive power. The experimental setup photo is shown in Fig. 15.
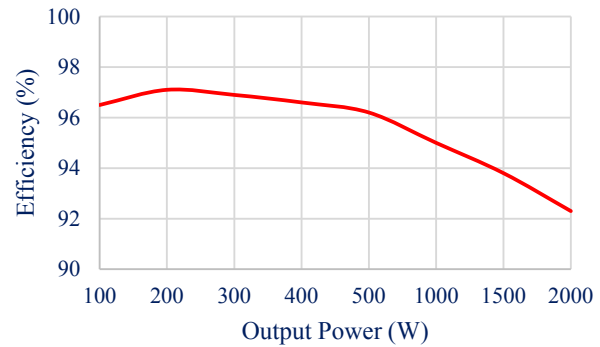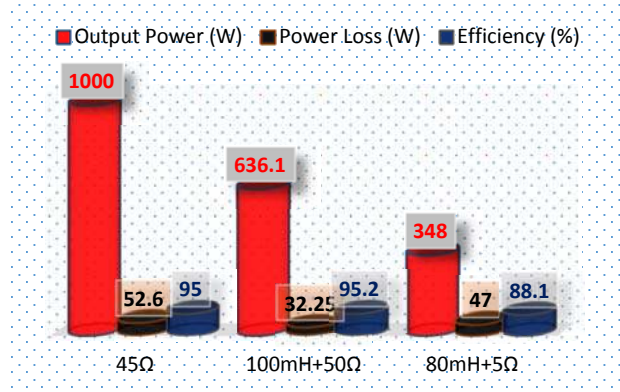
FIGURE 14 (a) Efficiency vs output power curve and (b) output power, power loss and efficiency with different loading conditio

8

IEEE Access·

Saeed A, J. Sathik, D. Almakhles, Abdulaziz A, Mohammed O
Seven Level T-Type Switched Capacitor Inverter-Rooftop PV Applications

The power loss breakdown of different components of the proposed topology has been given in Table VII. The switch pair (S_1, S_1') and (S_2, S_2') have the higher power losses as both switches are involved in the charging of the FC along with the generation of different voltage levels.
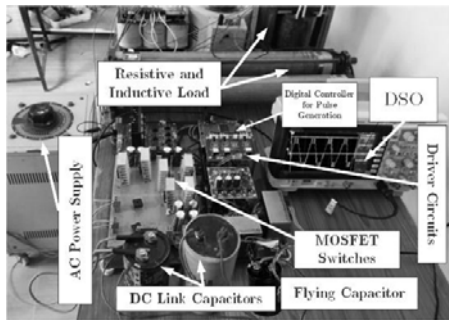

FIGURE 15 **Photo of Experimental Setup**

TABLE VII
POWER LOSS DISTRIBUTION OF THE PROPOSED TOPOLOGY WITH
$Z = 50\Omega + J100MH$

Power Loss of	P_{sw} (W)	P_c (W)	P_{loss} (W)
Switch S_1	0.1981	3.7901	3.9882
Switch S_1'	0.1923	3.7895	3.9818
Switch S_2	0.0705	4.4808	4.5513
Switch S_2'	0.1018	4.2647	4.3665
Switch S_3	0.0173	1.4601	1.4774
Switch S_3'	0.0158	1.2377	1.2535
Switch B_x	0.0749	1.0216	1.0965
Switch S_x	0.011	2.1105	2.1215
Total switch losses	0.6817	22.155	22.8367
Didoes			2.2023
Capacitors			7.2123

V. CONCLUSION

New topology of a seven-level switched capacitor inverter with self-voltage balancing and boosting has been presented in this paper. The proposed topology requires a lower number of power components with a maximum voltage of v_{in}. The sizing of capacitance is analyzed by selecting the longest discharging time duration. The comparison was carried out in this study which proved that the proposed topology overcomes the other recent SCMLI topologies presented in the literature. Further, in simulation, sudden load changes are applied and results are shown. The results show that the proposed topology is suitable for dynamic load varying applications and also due to the direct connection of the neutral to mid-point, this topology is more suitable for transformerless grid connected PV applications.

REFERENCES

1 S. Amamra, K. Meghriche, A. Cherifi and B. Francois, "Multilevel inverter topology for renewable energy grid integration", *IEEE Trans. Ind. Electron.*, vol. 64, no. 11, pp. 8855-8866, Nov. 2017.
2 R. R. Karasani, V. B. Borghate, P. M. Meshram, H. M. Suryawanshi and S. Sabyasachi, "A three-phase hybrid cascaded modular multilevel inverter for renewable energy environment", *IEEE Trans. Power Electron.*, vol. 32, no. 2, pp. 1070-1087, Feb. 2017.
3 N. Sandeep and U. R. Yaragatti, "Design and implementation of active neutral-point-clamped nine-level reduced device count inverter: An application to grid integrated renewable energy

sources", *IET Power Electron.*, vol. 11, no. 1, pp. 82-91, 2018.
4 K. Alluhaybi, I. Batarseh and H. Hu, "Comprehensive Review and Comparison of Single-Phase Grid-Tied Photovoltaic Microinverters," *IEEE J. Emerg. Sel. Topics Power Electron.*, vol. 8, no. 2, pp. 1310-1329, June 2020,
5 M. A Jagabar Sathik and K. Vijayakumar, "An assessment of recent multilevel inverter topologies with reduced power electronics components for renewable applications", Renewable Sustain. Energy Rev., vol. 82, no. 3, pp. 3379-3399, Feb. 2018.
6 M. Vijeh, M. Rezanejad, E. Samadaei and K. Bertilsson, "A General Review of Multilevel Inverters Based on Main Submodules: Structural Point of View," *IEEE Trans. Power Electron.*, vol. 34, no. 10, pp. 9479-9502, Oct. 2019.
7 H. Akagi, "Multilevel converters: Fundamental circuits and systems", *Proc. IEEE*, vol. 105, pp. 2048-2065, Nov. 2017.
8 J. Rodriguez, S. Bernet, P. K. Steimer and I. E. Lizama, "A survey on neutral-point-clamped inverters", *IEEE Trans. Ind. Electron.*, vol. 57, no. 7, pp. 2219-2230, Jul. 2010.
9 Y. Ye, K. Cheng, J. Liu and K. Ding, "A step-up switched-capacitor multilevel inverter with self-voltage balancing", *IEEE Trans. Ind. Electron.*, vol. 61, no. 12, pp. 6672-6680, Mar. 2014.
10 T. Roy, P. K. Sadhu and A. Dasgupta, "Cross-switched multilevel inverter using novel switched capacitor converters", *IEEE Trans. Ind. Electron.*, vol. 66, no. 11, pp. 8521-8532, Nov. 2019.
11 W. Peng, Q. Ni, X. Qiu and Y. Ye, "Seven-Level Inverter With Self-Balanced Switched-Capacitor and Its Cascaded Extension," *IEEE Trans. Power Electron.*, vol. 34, no. 12, pp. 11889-11896, Dec. 2019.
12 M. J. Sathik, K. Bhatnagar, N. Sandeep and F. Blaabjerg, "An improved seven-level PUC inverter topology with voltage boosting", *IEEE Trans. Circuits Syst. II Express Briefs*, vol. 67, no. 1, pp. 127-131, Jan. 2020.
13 W. Sheng and Q. Ge, "A Novel Seven-Level ANPC Converter Topology and Its Commutating Strategies," '*IEEE Trans. Power Electron.*, vol. 33, no. 9, pp. 7496-7509, Sept. 2018.
14 A. K. Yadav, K. Gopakumar, K. R. Raj, U. Loganathan, S. Bhattacharya and W. Jarzyna, "A hybrid seven-level inverter using low voltage devices and operation with single DC-link", *IEEE Trans. Power Electron.*, vol. 34, no. 10, pp. 9844-9853, Oct. 2019.
15 S. R. Pulikanti, G. Konstantinou and V. G. Agelidis, "Hybrid seven-level cascaded active neutral-point-clamped-based multilevel converter under SHE-PWM", *IEEE Trans. Ind. Electron.*, vol. 60, no. 11, pp. 4794-4804, Nov. 2013.
16 J. Liu, X. Zhu and J. Zeng, "A Seven-Level Inverter With Self-Balancing and Low-Voltage Stress," *IEEE J. Emerg. Sel. Top. Power Electron.*, vol. 8, no. 1, pp. 685-696, March 2020.
17 S. S. Lee and K.-B. Lee, "Dual-T-type seven-level boost active-neutral-point-clamped inverter", IEEE Trans. Power Electron., vol. 34, no. 7, pp. 6031-6035, Jul. 2019.
18 Y. Siwakoti, A. Mahajan, D. Rogers and F. Blaabjerg, "A novel seven-level active neutral-point-clamped converter with reduced active switching devices and DC-link voltage", *IEEE Trans. Power Electron.*, vol. 34, no. 11, pp. 10492-10508, Nov. 2019.
19 M. D. Siddique, S. Mekhilef, N. M. Shah, J. S. M. Ali and F. Blaabjerg, "A New Switched Capacitor 7L Inverter With Triple Voltage Gain and Low Voltage Stress," *IEEE Trans. Circuits Syst. II Exp. Briefs.*, vol. 67, no. 7, pp. 1294-1298, July 2020.
20 H. Vahedi, M. Sharifzadeh and K. Al-Haddad, "Modified Seven-Level Pack U-Cell Inverter for Photovoltaic Applications," *IEEE J. Emerg. Sel. Top. Power Electron.*, vol. 6, no. 3, pp. 1508-1516, Sept. 2018.
21 J. Zeng, W. Lin and J. Liu, "Switched-capacitor-based active-neutral-point-clamped seven-level inverter with natural balance and boost ability", *IEEE Access,* vol. 7, pp. 126889-126896, 2019.
22 M. D. Siddique, S. Mekhilef, N. M. Shah and M. A. Memon, "Optimal Design of a New Cascaded Multilevel Inverter Topology With Reduced Switch Count," IEEE Access, vol. 7, pp. 24498-24510, 2019.
23 M. D. Siddique, S. Mekhilef, N. M. Shah, A. Sarwar, A. Iqbal and

M. A. Memon, "A New Multilevel Inverter Topology With Reduce Switch Count," IEEE Access, vol. 7, pp. 58584-58594, 2019.

24 M. J. Sathik, N. Sandeep, M. D. Siddique, D. Almakhles and S. Mekhilef, "Compact Seven-Level Boost Type Inverter Topology," *IEEE Trans. Circuits Syst. II Express Briefs*, doi: 10.1109/TCSII.2020.3039387.

SAEED ALYAMI (M-) received the B.S. degree in electrical engineering from the King Fahd University of Petroleum and Minerals, Dhahran, Saudi Arabia, in 2004. Received the M.S. and PhD degrees in electrical and computer engineering from Wayne State University, Detroit, MI, USA, in 2010 and 2016 respectively. He is currently working as assistant professor at Majmaah University. From 2004 to 2008, he was a Power Transmission Engineer at the Engineering and Design Department for Substations and Grid Integration, in Saudi Electricity Company, Saudi Arabia. His research interests include smart grid, control of renewable energy system, and distributed generation.

JAGABAR SATHIK MOHAMED ALI (M-15, SM-19) was born in Madukkur, India, in 1979. He received the B.E. degree in electronics and communication engineering from Madurai Kamarajar University, Madurai, India, in 2002, and the M.E. and PhD degrees from the Faculty of Electrical Engineering, Anna University, Chennai, India, in 2004 and 2016, respectively. He is currently a postdoc fellow with the Renewable Energy Lab, College of Engineering, Prince Sultan University, Riyadh, Saudi Arabia. He is consultant of various power electronics companies for the design of power electronics converters. He has authored more than 40 articles publications in international journals and conference proceedings. His current research interests include multilevel inverters, grid-connected inverters, and power electronics converters and its applications to renewable energy systems. He is the receipt of certificate of recognition for second highest paper published in the year of 2019 and 2020 under IEEE-Madras Section.

DHAFER ALMAKHLES (M'14) received B.E. degree in Electrical Engineering from King Fahd University of Petroleum and Minerals, Dhahran, Saudi Arabia in 2006 and completed his Masters degree (Hons.) and his PhD from The University of Auckland, New Zealand in 2011 and 2016, respectively. Since 2016, he has been with Prince Sultan University - Saudi Arabia, where he is currently the chairman of the Communications and Networks Engineering Department and the Director of Science and Technology Unit. He is the leader for Renewable Energy Laboratory at Prince Sultan University. He has authored many published articles in the area of control systems. He served as a reviewer for many journals including IEEE Transactions on

Fuzzy Systems, Control of Network Systems, Industrial Electronics, Control Systems Technology and IEEE Control Systems Letters and International Journal of Control. His research interests include the hardware implementation of control theory, signal processing, networked control systems, nonlinear control design, unmanned aerial vehicle (UAV) and renewable energy.

ABDULAZIZ ALMUTAIRI is an assistant Professor in the Electrical Department, Majmmah University, KSA. He received the B.Sc. degree in electrical engineering from Qassim University, Buraydah, Saudi Arabia, in 2009, and the M.A.Sc. and Ph.D. degrees in electrical and computer engineering from the University of Waterloo, Waterloo, ON, Canada, in 2014 and 2018, respectively. His research involves both experimental studies and modeling of many system problems. His recent research activities focus on asset management in smart grids, power system reliability and resilience, and development of innovating techniques for integrating renewable energy resources and electric vehicle to power systems.

MOHAMMED OBEIDAT Received his PhD in Electrical Engineering from Wayne State University in 2013, M.Sc degree in Electrical Engineering was from Yarmouk University , Jordan in 2006, and B.Sc degree in Electrical Engineering from Jordan University of Science & Technology, Jordan in 1999. He is an Associate professor in power and mechatronics department at Tafila Technical University. He is a member of IEEE, Tau Beta PI Honor Society and Golden Key Honor Society. He was given the honor to be a Sigma Xi member from the Board of Governor, in 2012. He demonstrated excellent research and academic abilities as well as professional potentials. Dr. Obeidat has published several journal papers. Dr. Obeidat research of interest in the field of intelligent control systems, renewable energy, intelligent systems, and mechatronics.